AREAEE./ Rep.—278

ARAB REPUBLIC OF EGYPT
ATOMIC ENERGY ESTABLISHMENT
REACTOR AND NEUTRON PHYSICS DEPARTMENT

A MÖSSBAUER EFFECT SPECTROMETER

By
M.K. FAYEK
Y.M. ABBAS
A.A. BAHGAT

1983
NUCLEAR INFORMATION DEPARTMENT
ATOMIC ENERGY POST OFFICE
CAIRO, A.R.E.

AREAEE./Rep.-278

ARAB REPUBLIC OF EGYPT
ATOMIC ENERGY ESTABLISHMENT
REACTOR AND NEUTRON PHYSICS DEPARTMENT

A MOSSBAUER EFFECT SPECTROMETER

By

M.K. FAYEK
Y.M. ABBAS *
A.A. BAHGAT *

1983

NUCLEAR INFORMATION DEPARTMENT
ATOMIC ENERGY POST OFFICE
CAIRO, A.R.E.

* Guest scientist from Al-Azahr university

CONTENTS

ABSTRACT

A Mossbauer effect spectrometer of Harwell type is installed and put in operation. The driving system is of a constant acceleration mode with a velocity range 40mm/sec. and associated to a 1024 multichannel analyser, working in a multiscalar time mode. The gamma ray sources are 50 mCi Co^{57} in Pd and 20 mCi Sn^{119m} in Ba Sn O_3. Measurements are taken with the source kept at room temperature, while the absorber can be maintained at various temperatures. Gamma ray resonance spectra of different standard samples are obtained. Zero velocity and magnetic field calibration curves are deduced. Examples of some Mossbauer spectra for runing investigated materials with a comprehensive general description are also given.

I. INTRODUCTION

The Mossbauer effect (ME) is the name given to an aspect of the resonance absorption of gamma rays which was discovered by R.L. Mossbauer in 1958. The resonant absorption of the light emitted from excited atoms by other atoms of the same element is well known, and it might be expected that the same phenomenon should occur for nuclear gamma rays. However, in general this is not so and the reason becomes clear, when one considers the recoil energy and the line width in the two cases. The recoil energy is given by $R=\frac{E^2}{2Mc^2}$ where E is the photon energy and M the mass of the emitting atom. For an optical photon, R may be about 10^{-11} ev, but for a gamma ray, it is about 10^{-1} ev. The width of the resonance is given by the reciprocal of lifetime of the excited state and may be about 10^{-8} ev for an optical photon and about the same or somewhat broader for gamma rays. Thus, in one case, the recoil energy can be neglected, whereas in the other it is large enough to completely destroy the resonance condition. The same is true of the Doppler broadening produced by thermal vibration. The essence of the Mossbauer effect lies in a recognition of the changed circumstances, when the atom is bound in a lattice and the gamma ray energy is low so that the recoil energy is low compared with the crystal binding energies. Under these circumstances, Mossbauer was able to show that a fraction of the gamma rays f, are emitted free of the effects of recoil energy and Doppler broadening and are, therefore, able to be resonantly absorbed by other identical nuclei. The fraction f called the Mossbauer frac-

tion and is given by:

$$f = \exp \frac{-4\pi \langle X \rangle}{\lambda^2}$$

where X is the mean square vibrational amplitude of the omitting (or abosorbing) nucleus in the solid.

λ is the wavelength of the gamma photon.

The great value of the Mossbauer effect lies in the fact that the widths of the nuclear levels are often smaller than the interactions between the nucleus and the atomic electrons called the hypefine interactions. The strength and nature of these interactions depend strongly on the electronic, chemical and magnetic state of the atom. Thus, a spectrum of the nuclear resonant frequencies can give valuable information about the atom and its surroundings.

To explain the Mossbauer spectrum, some nuclear properties must be understood. The nucleus can be represented by a charge surronded by an electron cloud. The interaction between the electron colud and the nuclear charge can change the energies of the nuclear states. The difference in energy between the ground and excited nuclear states of the absorbers with respect to this difference in the source, is called the Isomer shift (IS) (fig. 1), measured in velocity units, generally centimeters per second, IS is related to the characteristics of the nucleus.

In general, the nuclear charge is not uniformly distributed. If the electron cloud is also not uniform, then an interaction occurs which splits the Mossbauer absorption line. This is called quadrupole splitting (Δ Eq) and arises when the nucelus is an electric field where direction and value change, as distance from the nucleus changes. This electric field gradient causes splitting in the level, i.e. of the excited nucleus. If the level is split in two, then two transitons can occur, giving two peaks (fig. 1). This splitting can be greatly affected by the type of bonding in which the element is involved.

The nucleus also has a magnetic field associated with it, which can cause nuclear energy levels to split further. Each level of spin quantum number I will split into (2I+1) sublevels, just as in the chmically more familiar case of unpaired extranuclear electrons. Transitions between these sublevels are governed by selection rule: $\Delta m_I = 0, \pm 1$
For iron nuclei, the selection rule gives rise to six lines as indicated in Fig.(2).

In most magnetic substances, the iron atom does not occupy a site with cubic point symmetry and a quadrupole splitting, as well as the magnetic splitting, will arise because the magnetic interaction is much stronger than the electric interaction and each of the energy sub levels will be shifted by a value corresponding to the electric interaction, as shown in Fig.(3).

More details about Mossbauer effect are given in a number of excellent articles and books which describe the basic aspects and sophisticated applications of this technique (1 - 10).

II. DESCRIPTION OF THE MOSSBAUER EFFECT SPECTROMETER

The ME spectrometer is composed of the following main parts (fig.4):

1) Gamma ray sources

Two gamma ray sources Co^{57} and Sn^{119m}, which are the most widely used isotopes, are available for measurements. Their recoilless fractions are sufficiently large for Mossbauer effect to be observed even at above room temperature.

(i) Co^{57} source (50 mCi) is diffused in a host palladium lattice, which is not self resonant and gives high recoilless fraction with no appreciable line broadening. The cobalt 57 decay scheme is given in fig. 5.

(ii) Sn^{119m} scurce of 20 mCi is embedded in a barium stannate matrix ($BaSnO_3$), such a matrix shows no line braodening, due to its unresolved quadrupole splitting; it also gives a large recoil free fraction at room temperature. Fig.(6) shows the decay scheme for Sn^{119m}. The reported parameters for 14.39 Kev gamma ray emitted from Co^{57}_{27}

isotope and 23.875 Kev gamma ray emitted from Sn_{50}^{119m} are given in (6).

2) The velocity transducer

In order to observe the Mossbauer effect, the gamma source should be given different small velocities. This is realized by mounting it on a system called the 'velocity transducer', it consists of:

(i) Vibrator

The vibration-generator consists of a moving coil, driver-compled to a moving magnet velocity-transducer and is connected to servo amplifier and waveform generator. It imparts to the source an acceleration which is constant to within 0.3% over the recorded range of velocities. The maximum velocity is 40 mm ces^{-1}. The stability of the drive is such that calibration need be infrequent. It is convenient to calibrate the drive, using an iron metal absorber and the linearity of the drive may be checked by measuring the differences between lines 1/2, 2/3, 4/5 and 5/6 which ideally should be equal in magnitude. The vibrator and the proportional counter, as well as the sample holder, are mounted on a table in the transmission geometry arrangement.

(ii) Servo-amplifier

A single width NIM module provides a drive to the

moving coil of the vibration generator and compares the unit waveform with the signal from the velocity pickup. The input is a differential amplifier, which permits the servo-amplifier to be used at a distance from the waveform generator, without suffering from interference. It also allows the scale to be reversed, so that the background curvature, which results from the inverse square law effect, can be eliminated when very small absorptions are under study and errors, due to non-linearities of the velocity scale, can be further reduced. The loop gain is sufficient to give a differential non-linearity of less than 0.3% with the standard vibration generator.

(iii) Waveform generator

A single width NIM module provides the servo-amplifier with a synchronised wave form and consists of a ramp running linearly from-v to +v, then returns to -v by two parabolas, i.e. the end of wave is returned to the starting point by a curve, so that the first two derivations (the acceleration and the change of acceleration) of the entire waveform are continuous in time. Two output pulses are also provided from the wave generator ('start' and 'address advance') in order to drive the multichannel analyser(Inotech type 1024) in the external multiscaling mode. Here, the analyser is stepped sequentially through its channels at a rate determined by the

address advance pulses are used to initiate the sequences.

a) Start 5V to 0, 0.2 μ sec seperated by 73 μ sec.
b) Address advance +5 to 0, 0.2 μ sec in trains of 512 pulses seperated by 100 μ sec.

3) Detection system

When the gamma rays fall on the absorber, they will suffer from the internal or external fields on the probe Fe nucleus and then come out affected by the characteristic features of the absorber. To observe these effects, the gamma rays coming out from the absorber are detected with a proportional counter. Harwell Mossbauer proprotional counter is desigend for counting 14.4 Kev gamma rays from Co^{57} and with operating voltage -218 Kv. The detecting medium is argon 10% methane, which gives efficiences of the order of 65% at 14.4 Kev, whilst providing good rejection of counts from the ten times more abundant 122 Kev gamma rays. The resolution at low counting rates is about 2 Kev full width at half maximum at 14.4 Kev and about 3 Kev at a count rate of 10^5 14.4 Kev gamma rays per second, using 0.2 μ sec differentiating and integrating time constants. Since the output inpedence of the detector is very high, a preamplifier is used, followed by a linear amplifier. The peak voltages of the pulses, produced by the linear amplifier, are proportional to the gamma ray energy. A single channel analyser is used to select only pulses above a threshold,

but in the window of the single channel analyser, so that the gamma ray energy can be selected. Logic pulses from the linear gate (SCA), signalling the detection of 14.4 Kev gamma ray, are stored in a 1024 channels pulse height analyser, which is divided into two 512 memory subgrouping operated as a multichannel scaler (operated in the time mode).

4) Measurements at low temperature

If the specimen displays the properties under investigation at low temperatures, the source may be at room temperature and a cryostat with suitable windows can be employed to hold the specimen. Fig.(7) shows a sectional view of the available liquid nitrogen cryostat. The outer PVC vacuum vessel is sealed to the inner stainless steel vessel by means of an O ring piston type seal. Both vessels are equipped with thin mylar windows (low absorption window material to allow the low energy radiation to reach the detector). The sample tube is brazed to the vacuum vessel. This serves to keep liquid refrigerant out of the sample tube, the lower part of which is copper. This is in contact with the refrigerant and surrounds the sample space, ensuring that it will be at refrigerant temperature. The sample is mounted on the holder and after precooling, it is inserted down the sample tube. To obtain spectra at

temperatures other than 77 K, the variable temperature is inserted and is used (Fig.7). The specimen is contained inside an evacuated cell and is heated by an electric heater.

III. CALIBRATION OF THE MOSSBAUER EFFECT SPECTROMETER

In order to derive the values of interaction parameters from a Mossbauer spectrum, one needs to know an energy scale against which it can be plotted. Two problems arise: The first is the determination of the zero point, and the second is the determination of the energy scale, relative to that point. It has became customary to give the energy in velocity units, so that the actual energy change involves the gamma ray energy. The energy introduced by the Doppler shift is given by:

$$E_D = \frac{v}{c} E_\gamma$$

In order to calibrate the present installed constant acceleration spectrometer, the following steps were taken:

1) Source calibration

Before using the multiscaling mode to measure a Mossbauer spectrum, it is necessary to bracket the required energy range in the pulse height spectrum in the PHA mode. This is done by feeding the main amplifier output to the input

connector on the analyser, with the PHA/MCS switch at PHA and operating the lower and upper discriminators,i.e. the amplifier pulse analyser must be set to count along the 14.4 Kev gamma rays from the source. This was achieved by

a) Setting the gain and the threshold in order to exclude the 6.4 Kev X-rays.

b) Setting the window to include the line width of the 14.4 Kev gamma rays.

c) An aluminium filter is used to decrease the count rate, correponding to the 6.3 Kev X-rays.

The plot of the number of counts/second as a function of the threshold was obtained similar to that in Fig.(4).

Generally, the gain setting is dependant on the characteristics of the proportional counter. After several hundred hours of use, ageing of the proportional counter tube will require a voltage increase.

2) Calibration standards

The first requirement in undertaking a relative calibration is the selection of a reference material having line positions which are reproducible, easily measured and universally agreed upon. Three standards with different magnetic ordering type were used for this purpose:

(i) Sodium nitroprusside:

Na_2 (Fe $(CN)_5$ NO)2 H_2O. The splitting of the 14.4 Kev level into two states by the electric field gradient at the nucleus, is easily observed in sodium niotroprusside (Fig.8) which has a pure quadrupole interaction. A suitable range of velocities, sufficient to observe the doublet pattern (20 dB) was used. The magnitude of the quadrupole splitting was calculated and the centre of the quadrupole adopted as the zero.

(ii) Metallic iron:

Fe^{57} foil, because of its high intrinsic magnetic field, is the most convenient standrad sample for calibration of chamical isomer shift and to observe the nuclear Zeeman effect. A Mossbauer spectrum for a standard iron foil with suitable velocity range was obtained (Fig.9). There are six hyperfine components giving a linearity check as well as defining a zero velocity (fig.11).

(iii) Fe_2O_3:

The obtained Mossbauer effect spectrum at room temperature (Fig.10) for this material has six lines, due to the superexchange interactions, acting on Fe^{57} single nucleus. It showe an isomer shift from natural iron, a larger magnetic field and a small quadrupole coupling with an electric field gradient.

The obtained parameters from the above standards are used for the calibration of both observed velocities and hyperfine fields, as shown in Figs. 11 and 12).

IV. EXAMPLES OF RUNNING ME MEASUREMENTS

(i) The determination of the microscopic arrangement of atomic magnetic moments in a crystal lattice is often of interest because the macroscopic magnetic properties are related to the magnetic structure in much the same way as other physical properties are related to the crystal structure. In the cases where the hyperfine field is parallel or antiparallel to the atomic magnetic moment, as for example in ionic Fe^{3+}, where the hyperfine field primarily originates from the core polarization magnetic field, Mossbauer spectroscopy can be used to determine the direction of the internal magnetic field, relative to the crystal axes and thus the spin direction. Measurements on two different magnetic compounds are considered:

a) The cubic ferrites $Cd_X Mg_{1-X} Fe_2O_4$ are ferrimagnetic up to the composition with $X \leq 0.5$. On the other hand, $CdFe_2O_4$ is antiferromagnetic. There is a lack of data of the magnetic behaviour of the compositions between $X \approx 0.5$ and the stoichiometric Cd-ferrite. Therefore, ten samples of the formula $Cd_X Mg_{1-X} Fe_2O_4$ with different X values are prepared, aiming to dete-

rmine cation distribution and the magnetic type ordering in these compounds. An example of the Fe^{57} Mossbauer measurements is given in Fig.(13) for one of these compounds ($MgFe_2O_4$) at room temperature. The observed asymmetric lineshape is ascribed to the presence of two distinct hyperfine fields, related to tetrahedral A and octahedral B sites which, however, could not be resolved. A detailed study of the whole system at different temperatures is now in progress.

b) Fe^{57} Mossbauer effect spectra are obtained for three powder smaples of the alkaline earth ferrites $Ba\ Sr_x\ Ca_{1-X}\ Fe_4O_8$, aiming to provide information on the changes occuring at the Mossbauer atom site, and the magnetic ordering in these compounds. The spectra of these monoferrites are magnetically split, indicating antiferromagnetism at room temperature. A simple six lines spectrum of the compound with $X=0.5$ is shown in Fig.(14). Results of Mossbauer effect and neutron diffraction measurements on these compounds, are published in a separate report.

(ii) The assignment of the oxidation state of iron or the ratio of oxidation states, is of considerable geological importance in explaining such phenomena as colour, pleochroism, oxidation and weathering of minerals. Figs.(15 and 16) show the Fe^{57} Mossbauer spectra of two powder samples

of iron bearing minerals (taken from east and west desert of Egypt). The first spectrum is related to hematite ore in a weak ferrimagnetic state and with its familiar Mossbauer parameters at room temperature, where there are six lines due to the superexchange interactions, acting on Fe^{57} single nucleus. The second spectrum (Fig.16) is of a basalt sample, its Mossbauer parameters identify clearly the iron in its ferrous and ferric states. Areas of the two subpatterns reflect the Fe^{2+}/Fe^{3+} ratio.

(iii) The amorphous metal ($T_{80}M_{20}$) alloys, where T (transition metal) = Fe,Co, Ni, Pd, Mo and M (metalloid) = B, C, N, P and Si, has received nowadays considerable attention because of its potential technological importance. These amorphous metals are sold under the trade name metaglass. In general, the composition range of the relative stable glassy state is found in the vicinity of 80 at % metal and 20 at % metalloid. It should be mentioned that a large variety of amorphous metals exists, however, so far rather scarce information has been extracted from Mossbauer spectroscopy and published in the literature. Mossbauer effect spectra at room temperature are obtained for two amorphous metal samples 2826 MB (Fe_{40} Ni_{38} Mo_4 B_{18}) and 2605 SC (Fe_{81} $B_{13.5}$ $Si_{3.5}$ C_2), kindly supplied by 'Allied Chemical' (fig.17). These ferromagentic amorphous alloys exhibit very similar spectra

each hyperfine pattern has very broad lines, which indicate a distribution of hyperfine fields. The lack of resolution of the spectral lines may lead to the application of different models for the fitting and interpretation of the spectra and the distribution of fields. Further measurements and intense study on such alloys are now in progress..

(iv) Sn^{119} Mossbauer effect spectrum for the balck SnO is obtained at room temperature with suitable range of velocity (Fig.18). The spectrum has the characteristic parameters (isomer shift and quadrupole splitting). SnO is tetragonal and the resultant asymmetry in the quadrupole splitting shows that e^2 qQ is positive and lies along the crystal axis. The tin atom has four equidistant oxygen neighbours which form the corners of a square, the tin itself being at the apex of a square pyramid.

FIGURE CAPTIONS

Fig. 1: Electric quadrupole splitting in sodium nitroprusside.

Fig. 2: Magnetic splitting of nuclear levels in Fe^{57}.

Fig. 3: Hyperfine splitting of nuclear energy levels, showing electric quadrupole perturbation of hyperfine magnetic dipole interaction(the case of Fe_2O_3).

Fig. 4: A block diagram of the Mossbauer effect spectrometer.

Fig. 5: Co^{57} decay scheme.

Fig. 6: The decay scheme for Sn^{119}.

Fig. 7: a) A liquid nitrogen cryostat, the specimens are mounted on insulating rods which can be inserted in the central tube of the cryostat.

b) A specimen holder for variable temperature measurements where the specimen is electrically heated and the temperature controlled by an external controller.

Fig. 8: A Mossbauer effect spectrum of sodium nitroprusside at room temperature.

Fig. 9: A Mossbauer effect spectrum of metallic iron.

Fig.10: Gamma-ray resonance absorption of $-Fe_2O_3$.

Fig.11: Linear velocity calibration.

Fig.12: Magnetic hyperfine field calibration.

Fig.13: Fe^{57} Mossbauer spectrum of the spinel $MgFe_2O_4$ at room temperature.

Fig.14: ME spectrum of the monohexaferrite solid solution $Ba\ Sr_{0.5}Ca_{0.5}Fe_4O_8$.

Fig.15: Gamma ray resonance absorption spectrum of natural hematite iron ore.

Fig.16: A Mossbauer effect spectrum of Egyptian bazalt.

Fig.17: ME spectra of two metaglass alloys.

Fig.18: Sn^{119} Mossbauer effect spectrum of the balck stanous oxide.

REFERENCES

1) G.K. Wertheim: Mossbauer effect, principles and applications(Academic Press New York 1964).

2) I.J. Gruverman: Mossbauer effect methodology vols.1-9 (Plenum Press, New York 1965-1974).

3) V.I. Goldanskii and R.H. Herber:Chemical applications of Mossbauer spectroscopy(Academic Press New York 1968).

4) J.G. Stevens and V.E. Stevens: Mossbauer effect data index ((Plenum, New York, 4 volumes 1969-1972).

5) L. May: An introduction to Mossbauer spectroscopy (Plenum Press, New York 1971).

6) N.N. Greenwood and T.C. Gibb: Mossbauer spectroscopy (Chapman and Hall, London 1971).

7) G.M. Bancroft: Mossbauer spectroscopy. An introduction for inorganic chemists and geochemists (McGraw-Hill, London 1973).

8) T.E Cranshaw: Mossbauer spectroscopy J. Physics E 7, 497, 1974.

9) V. Gonser: Mossbauer spectroscopy topics in applied physics (Springer Verlag, Berlin 1975).

10) V. Gonser: Atomic energy review supplement No. 1 (1981) IAEA.

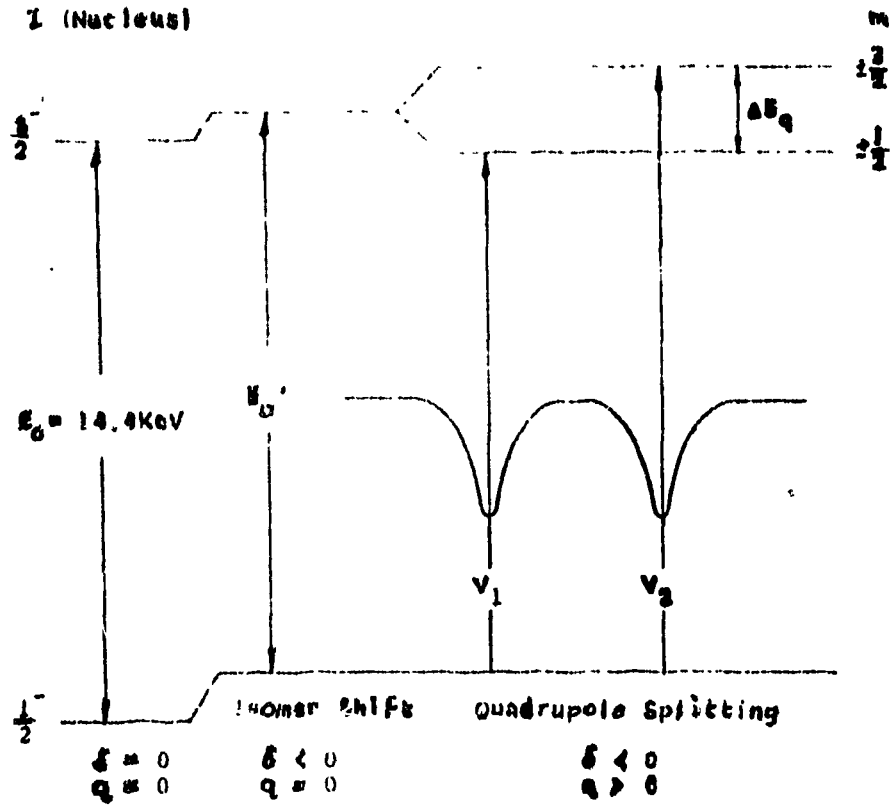
I (Nucleus)
m
$\pm\frac{3}{2}$
$\pm\frac{1}{2}$
$\frac{3}{2}^-$
$\frac{1}{2}^-$
ΔE_q
$E_\gamma = 14.4KeV$
E_γ'
V_1
V_2
Isomer shift
Quadrupole Splitting
$\delta = 0$ $q = 0$
$\delta < 0$ $q = 0$
$\delta < 0$ $q > 0$

Fig.1

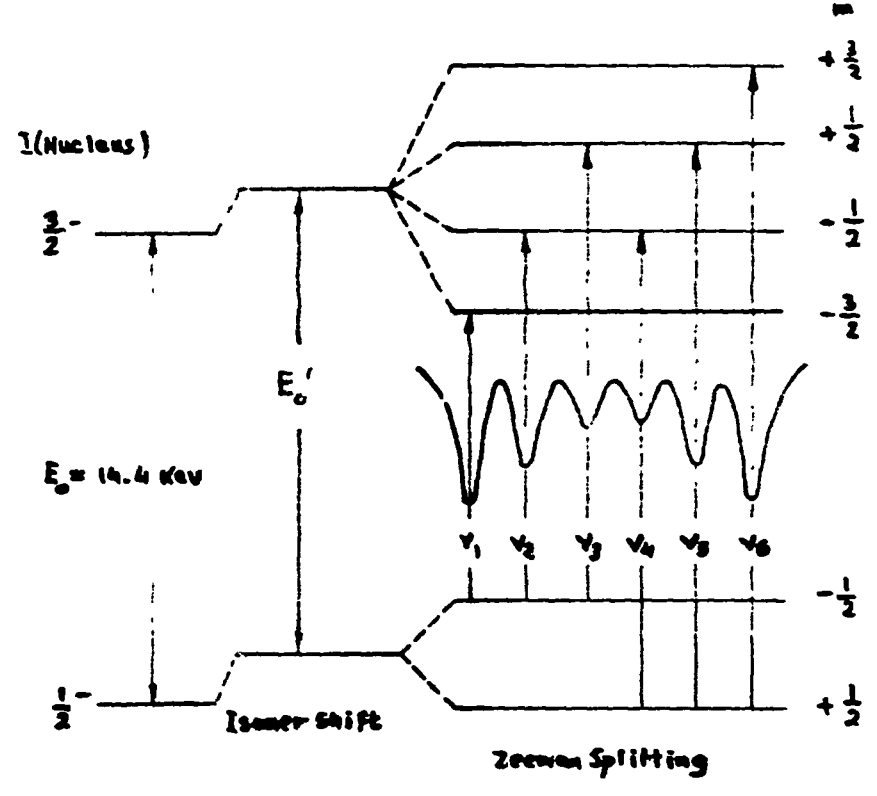
I(Nucleus)
3/2-
1/2-
E₀'
E₀ = 14.4 Kev
Isomer Shift
Zeeman Splitting
m
+3/2
+1/2
-1/2
-3/2
-1/2
+1/2
ν₁ ν₂ ν₃ ν₄ ν₅ ν₆

Fig. 2

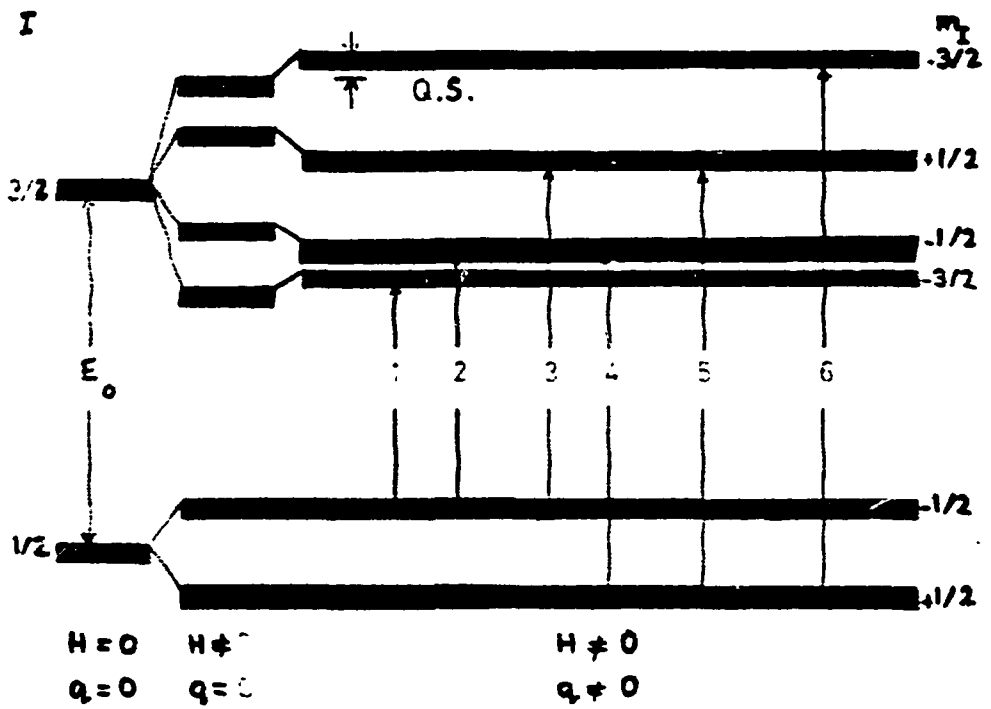
I
m_I
-3/2
Q.S.
+1/2
3/2
-1/2
-3/2
E_o
1
2
3
4
5
6
-1/2
1/2
+1/2
H=0
H≠
H≠0
q=0
q=
q≠0

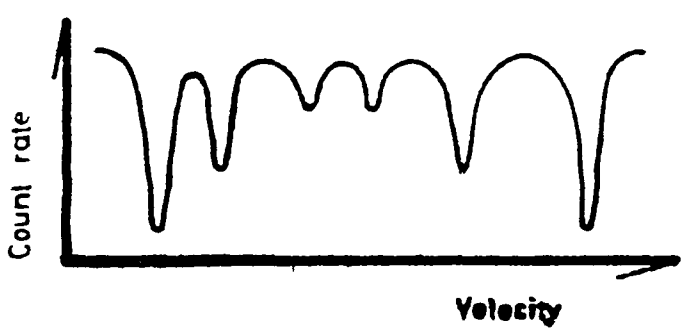
Count rate
Velocity

Fig.3

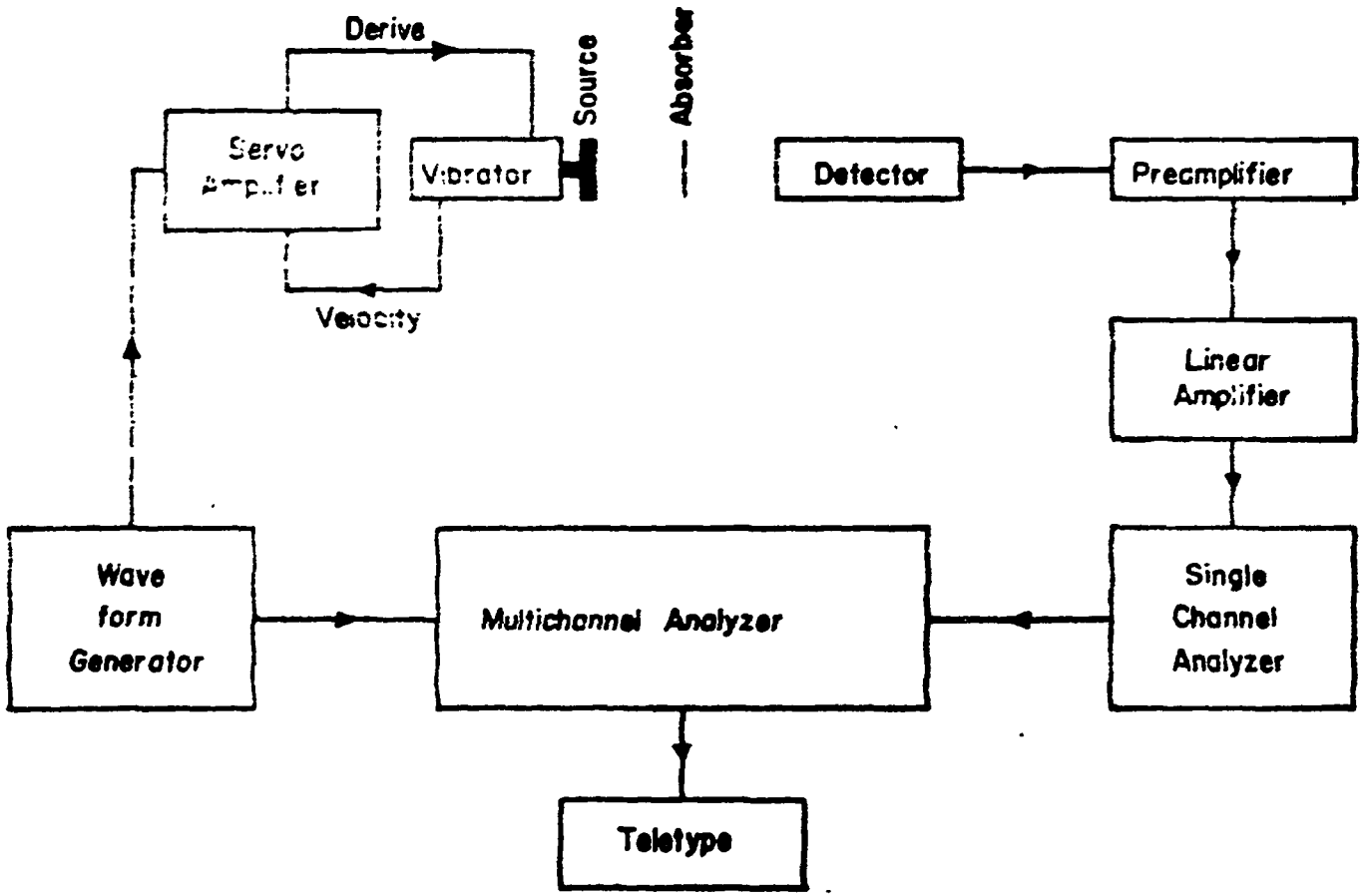
Derive
Source
Absorber
Servo
Amplifier
Vibrator
Velocity
Detector
Preamplifier
Linear
Amplifier
Wave
form
Generator
Multichannel Analyzer
Single
Channel
Analyzer
Teletype

Fig.4

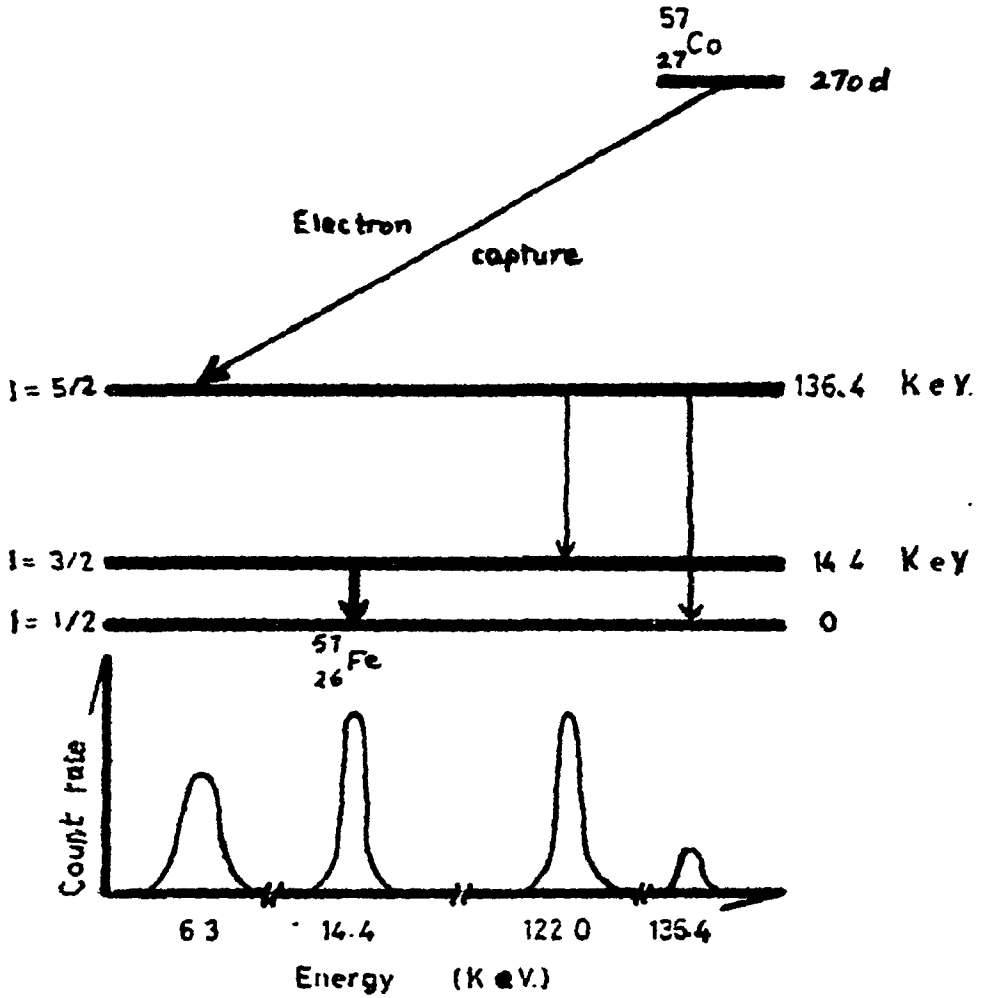
57 Co 27
270 d
Electron capture
I = 5/2
136.4 K e V.
I = 3/2
14 4 K e V
I = 1/2
0
57 Fe 26
Count rate
6 3
14.4
122 0
135.4
Energy (K e V.)

Fig.5

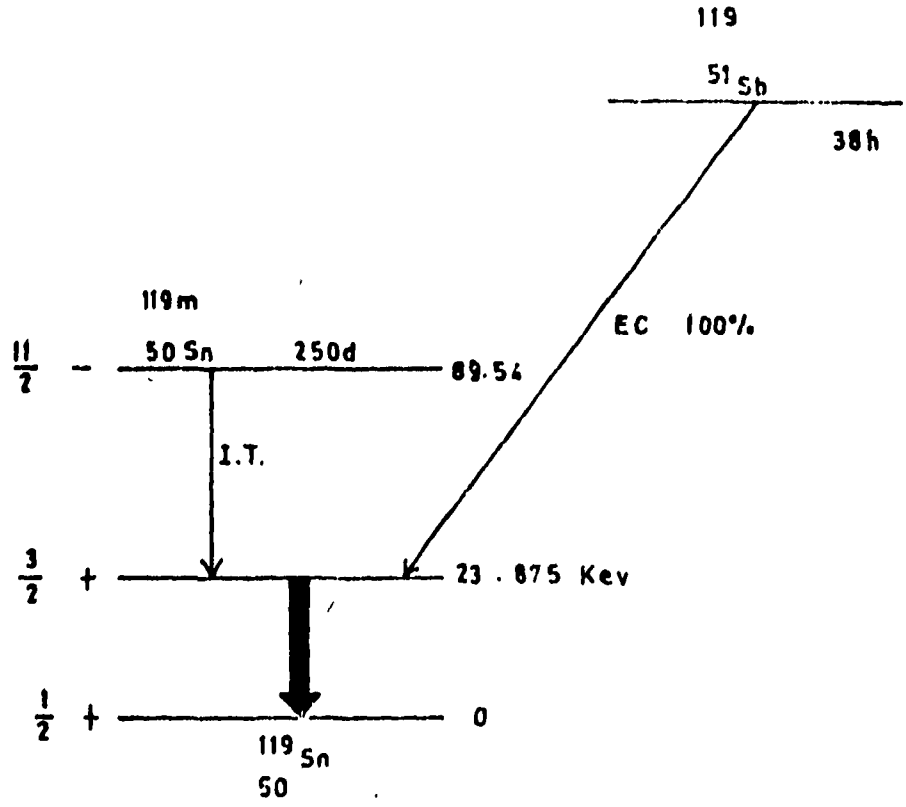
119
51 Sb
38h
119m
50 Sn
250d
11/2 −
89.54
EC 100%
I.T.
3/2 +
23.875 Kev
1/2 +
0
119 Sn
50

Fig.6

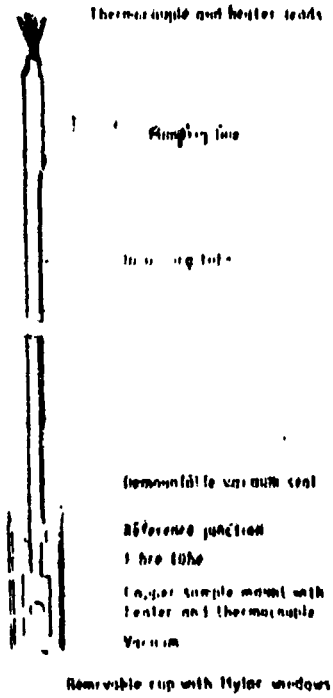

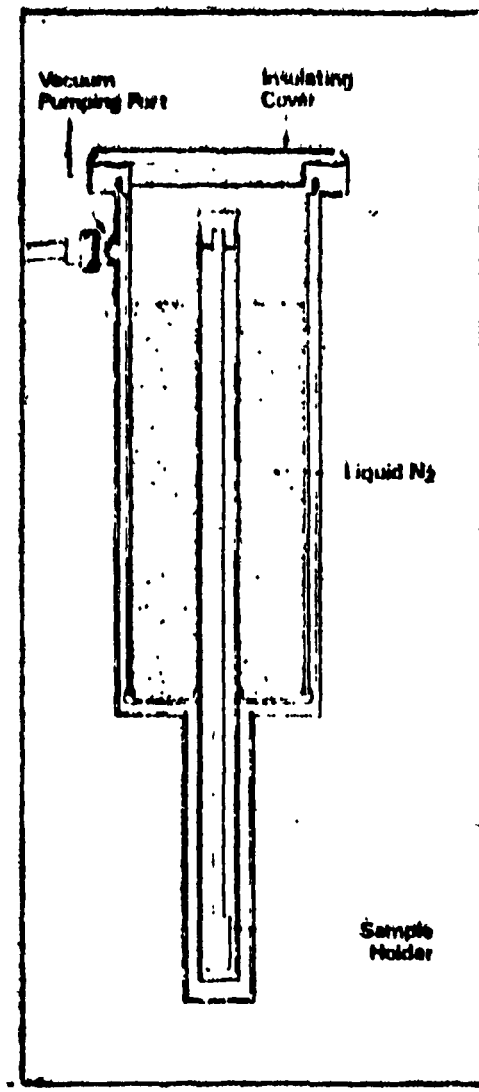
Vacuum
Pumping Port
Insulating
Cover
Liquid N2
Sample
Holder

Fig.7

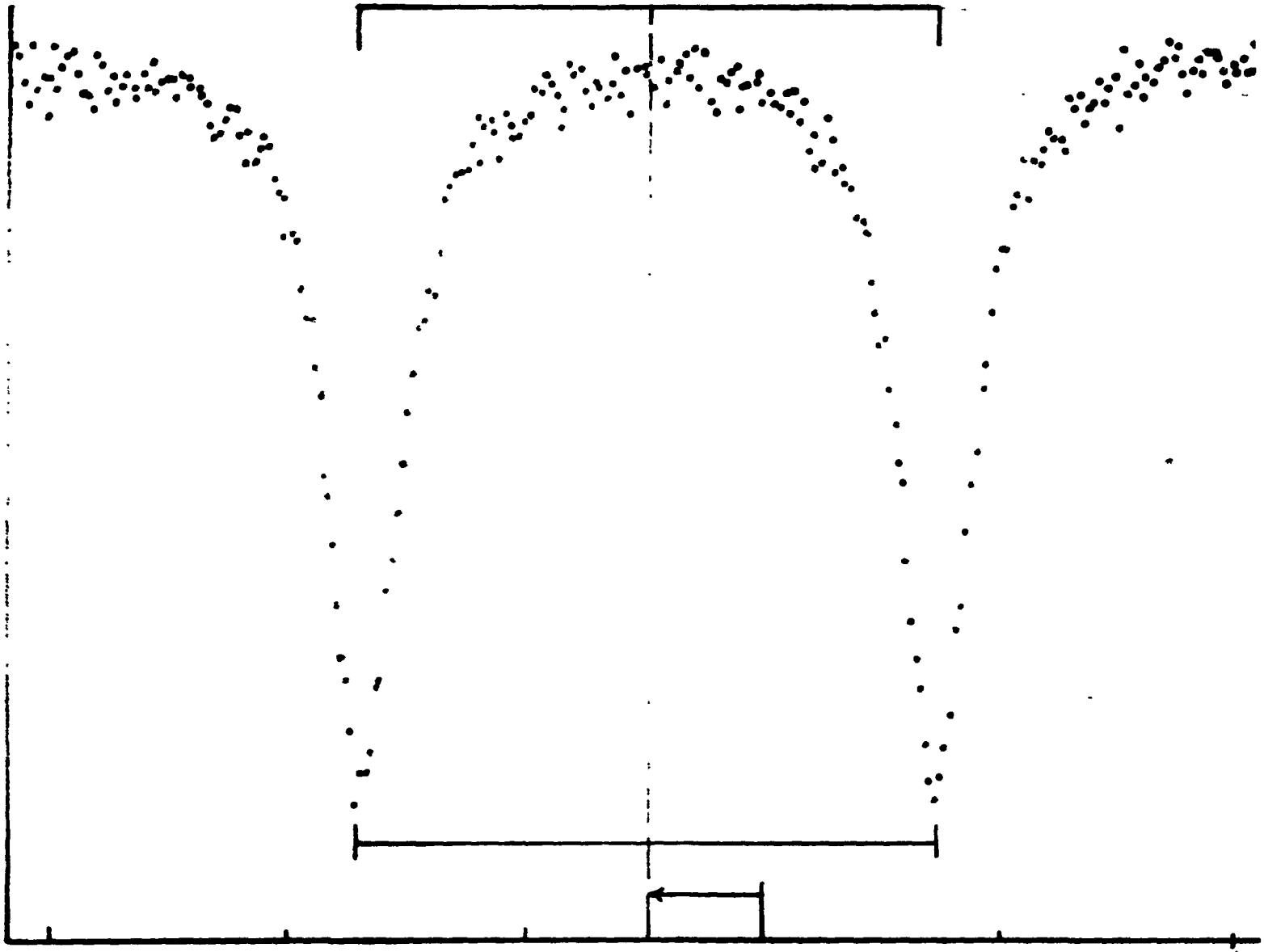

Fig. 8

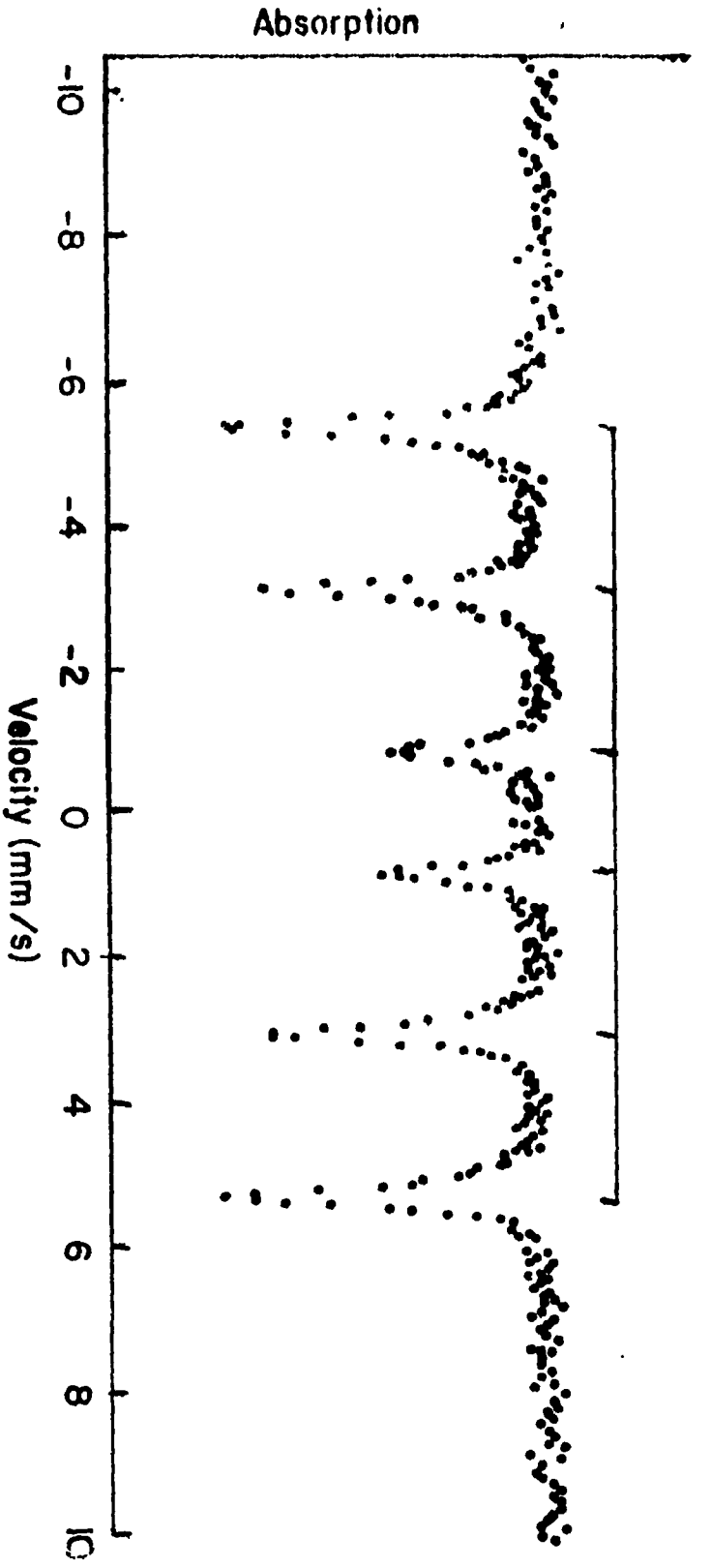

Fig. 9

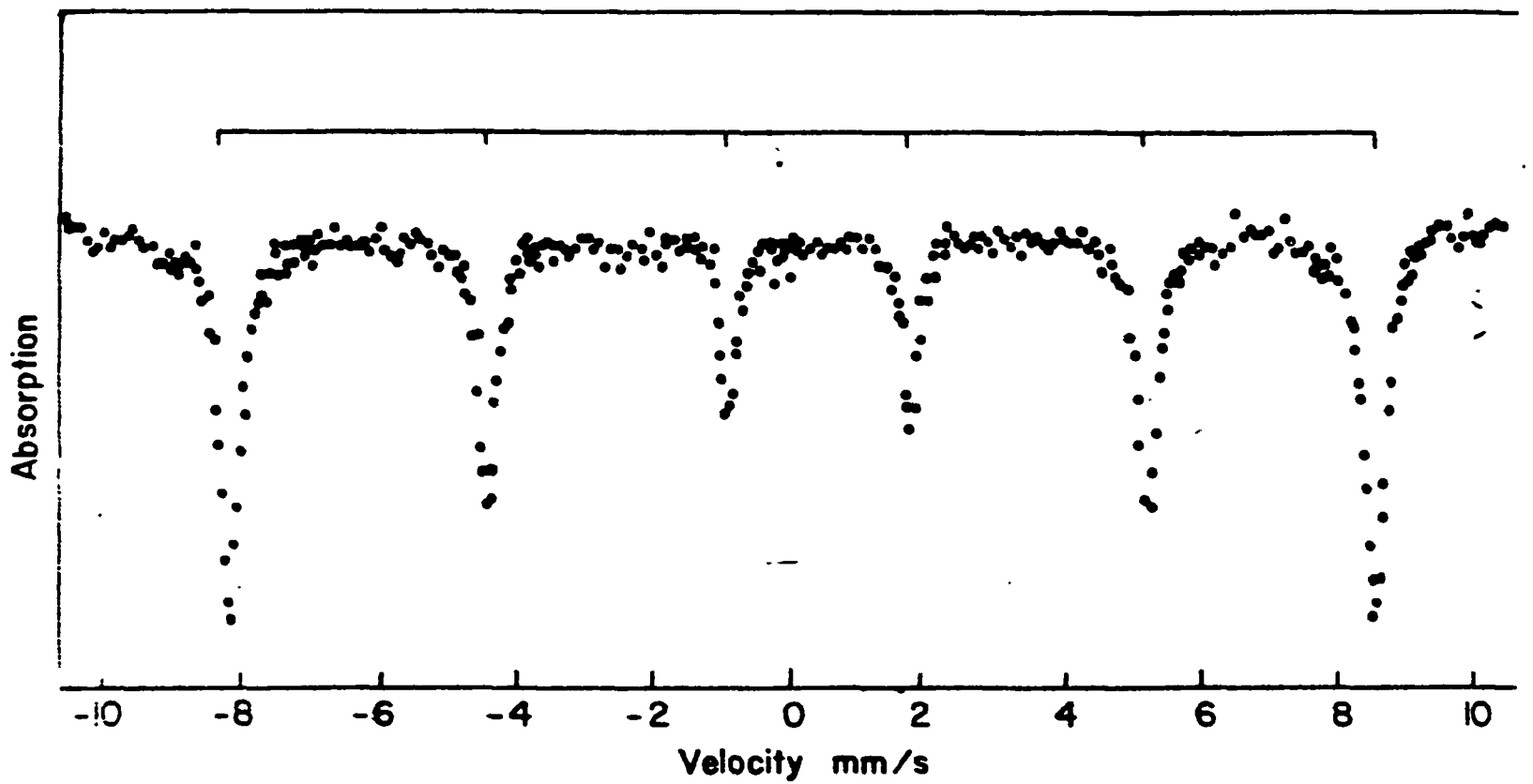

Fig. 10

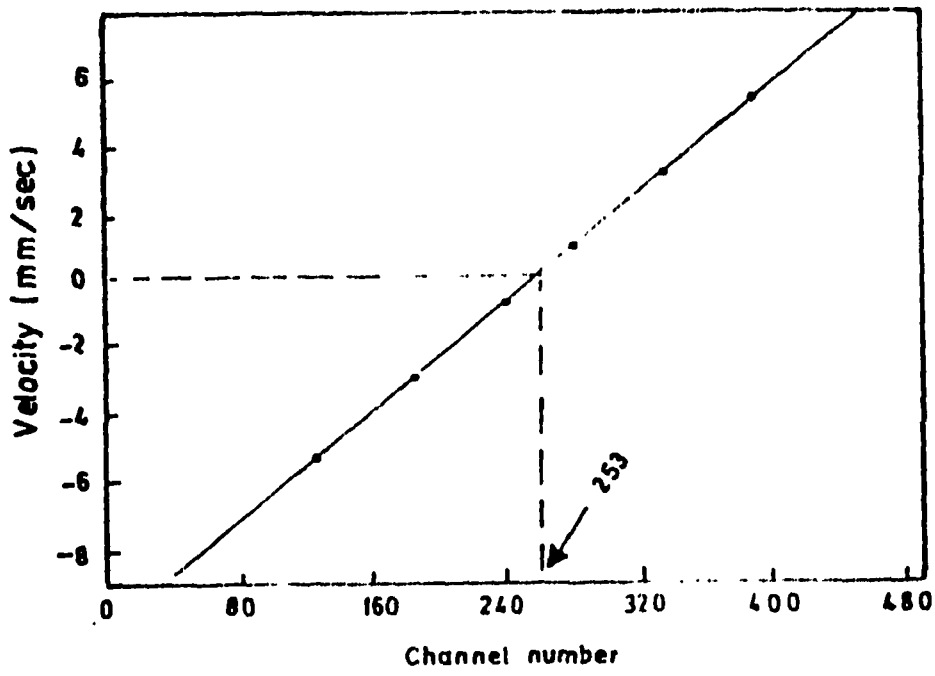
Velocity (mm/sec)
6
4
2
0
-2
-4
-6
-8
253
0
80
160
240
320
400
480
Channel number

Fig. 11

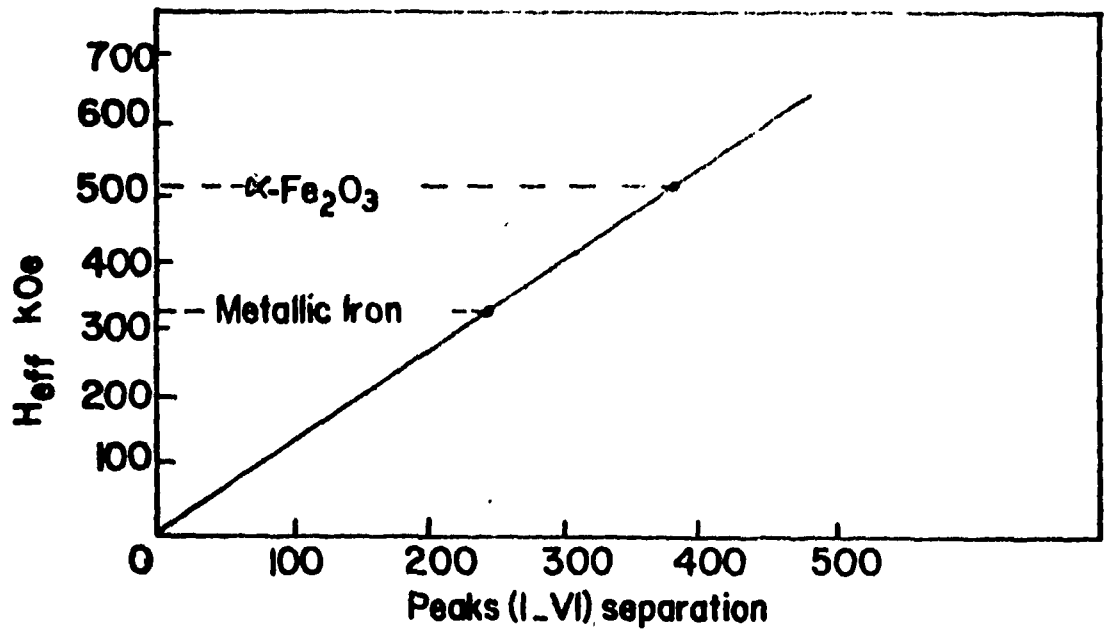
700
600
500
400
300
200
100
H_{eff} kOe
α-Fe_2O_3
Metallic iron
0
100
200
300
400
500
Peaks (I_VI) separation

Fig. 12

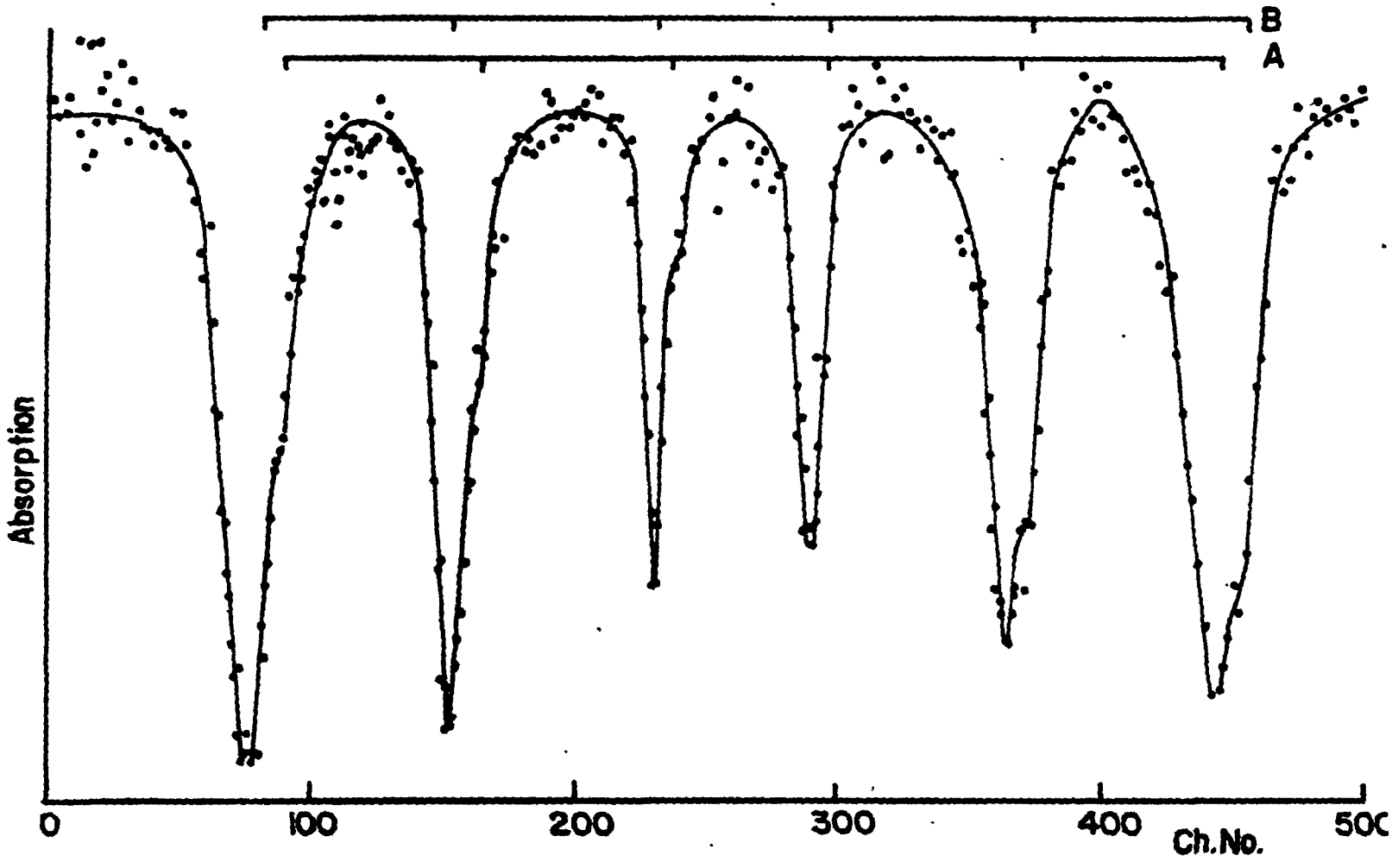

Fig. 13

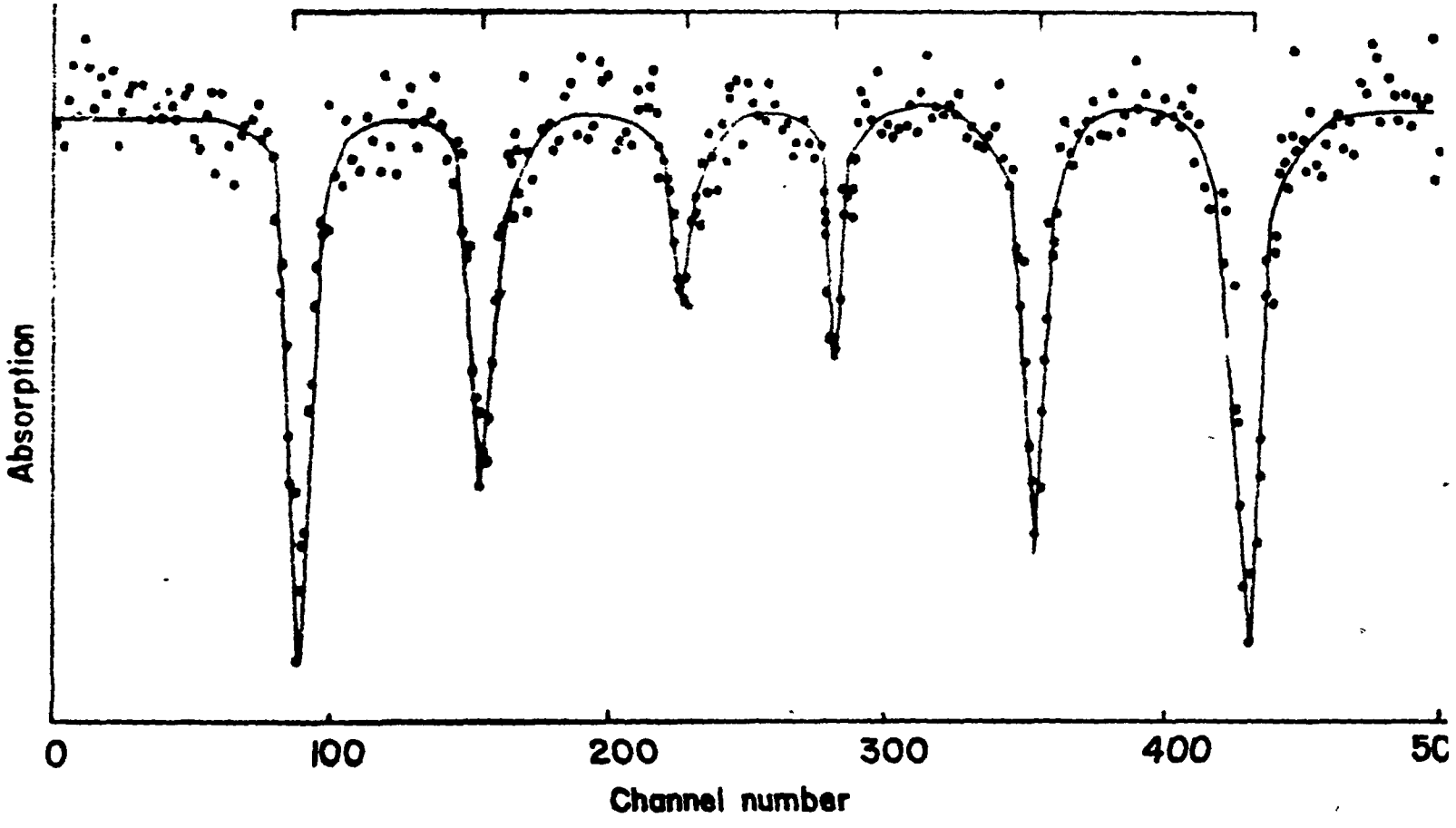

Fig. 14

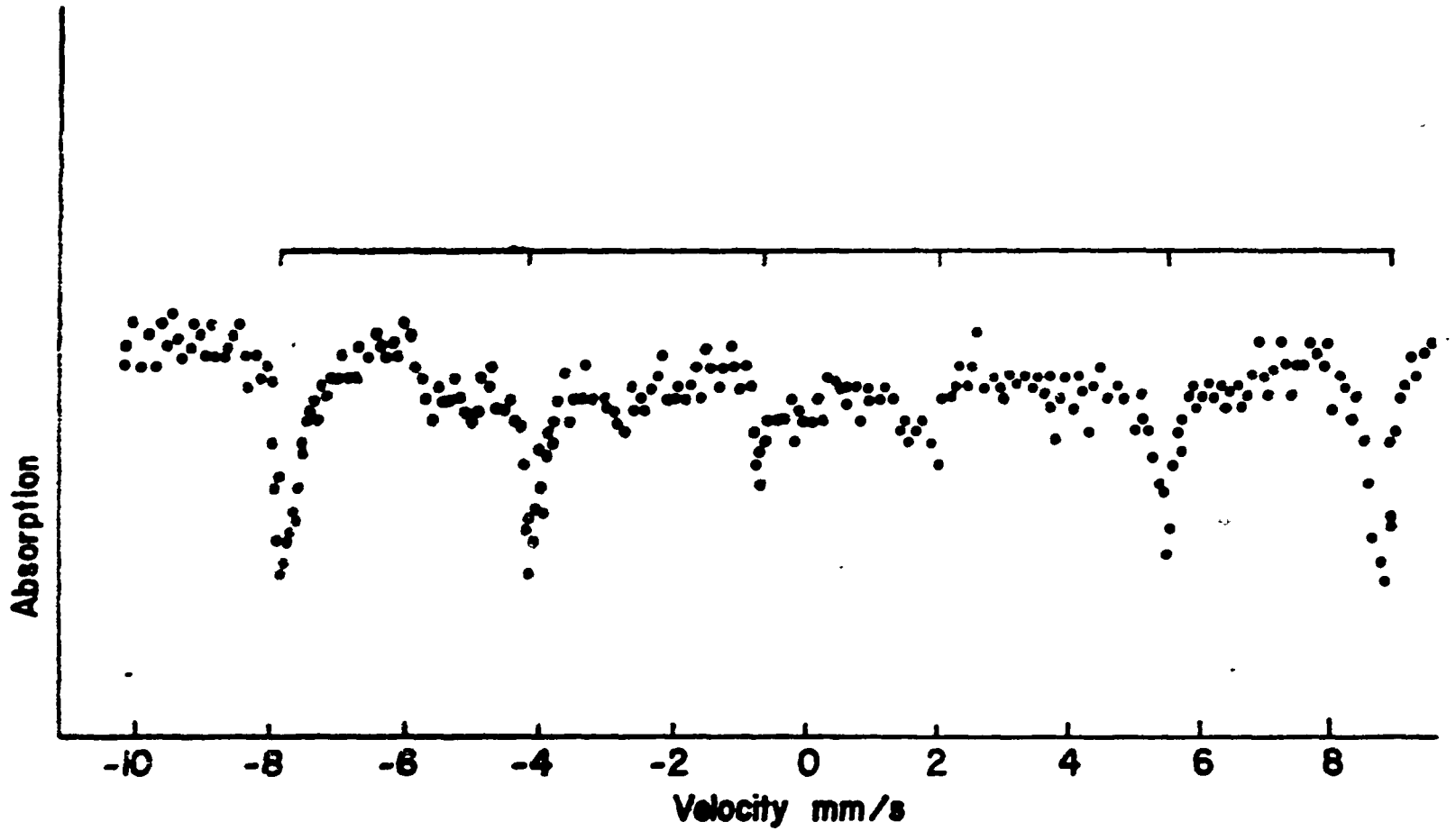

Fig.15

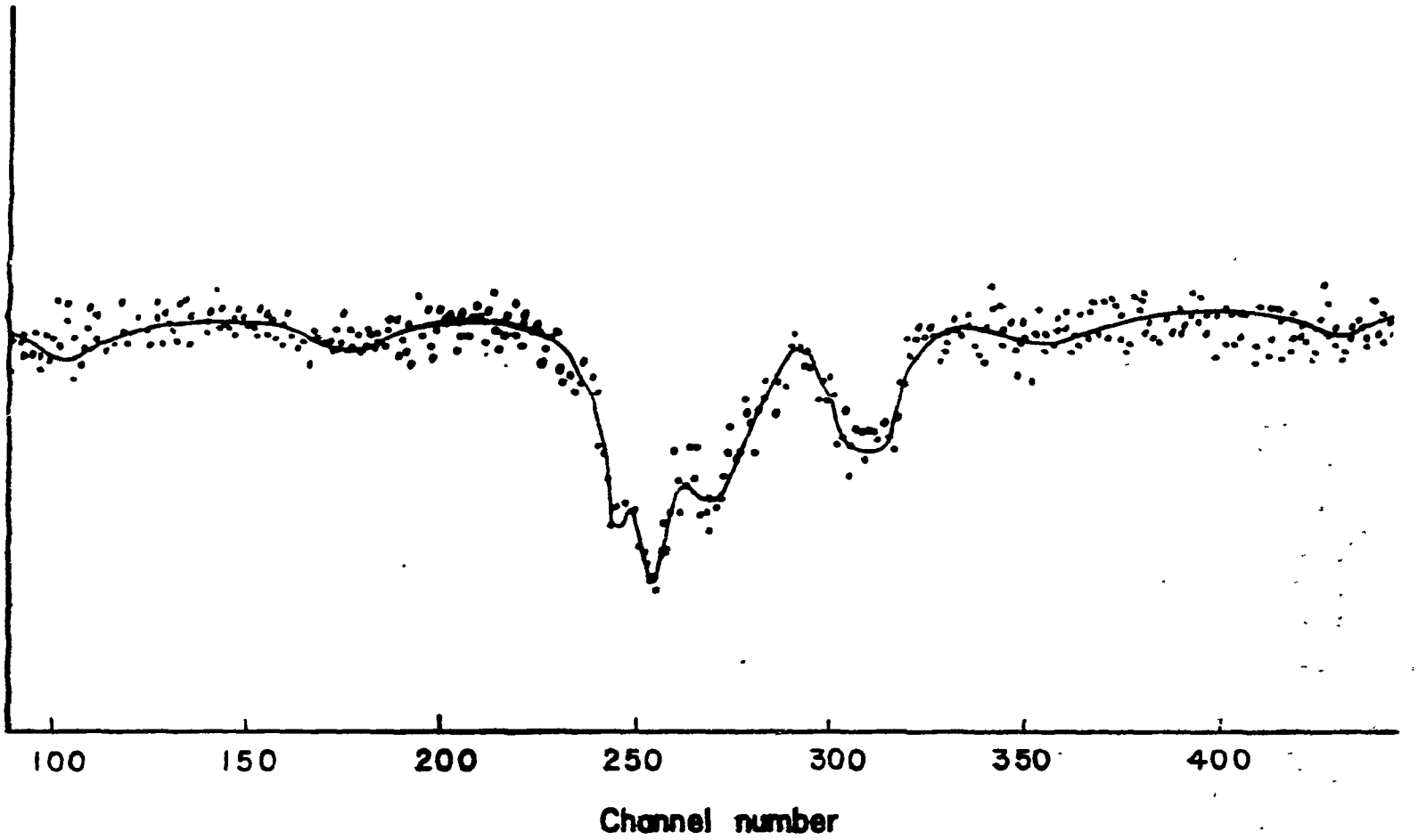

Fig. 16

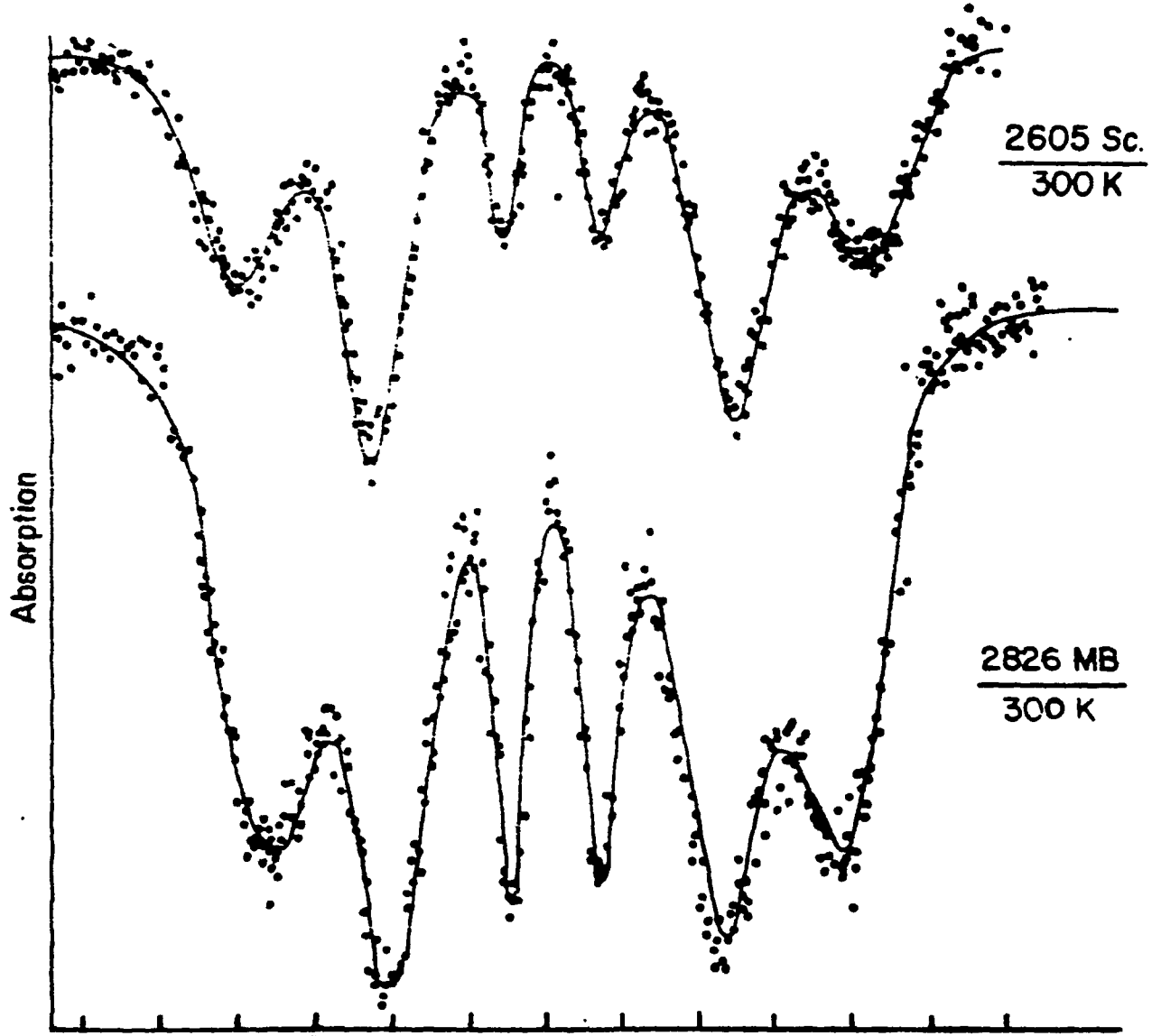

Fig. 17

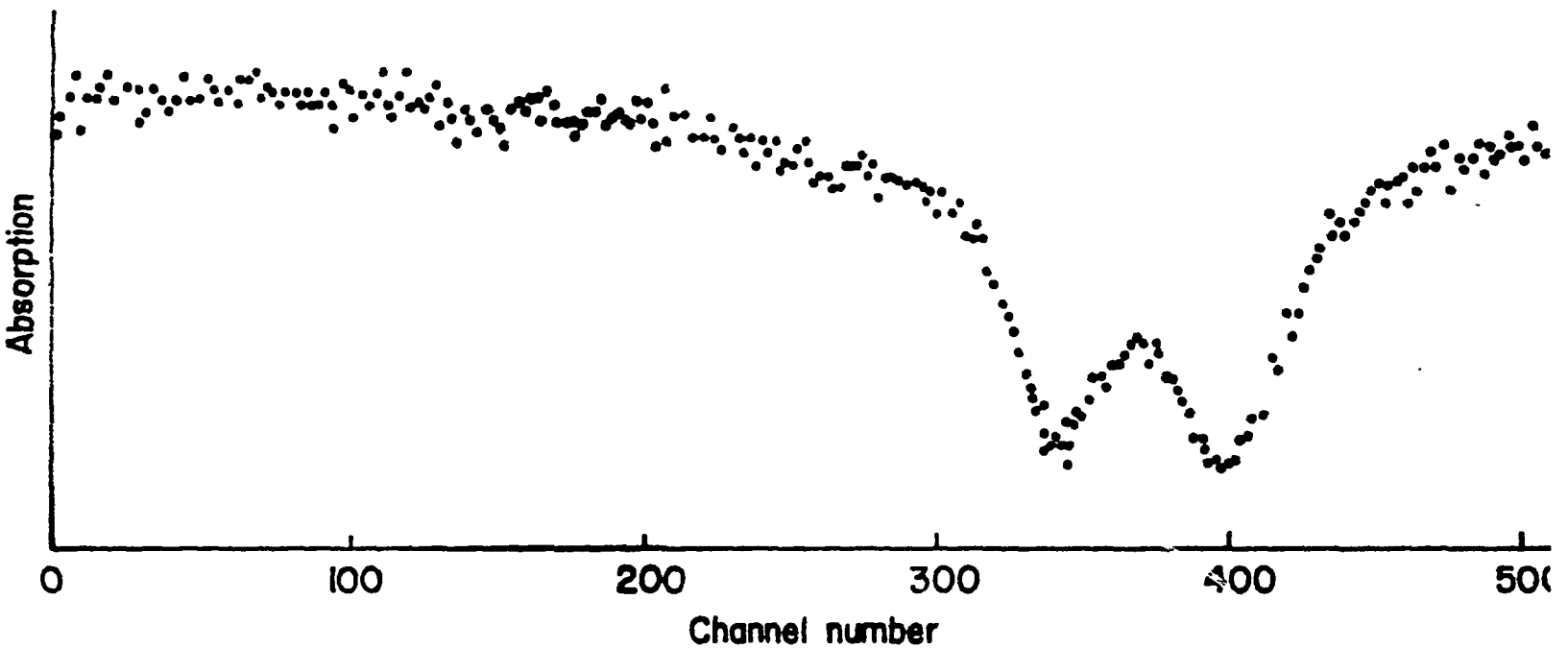

Fig. 18